JOURNAL OF APPLIED ELECTROCHEMISTRY **29** (1999) 59–63

Nanoparticles produced by borohydride reduction as precursors for metal hydride electrodes

M. MITOV

Department of Chemistry, South-West University, Blagoevgrad, Bulgaria

A. POPOV, I. DRAGIEVA

Central Laboratory of Electrochemical Power Sources, Bulgarian Academy of Sciences, Sofia, Bulgaria

Received 4 July 1997; accepted in revised form 24 February 1998

The performance of electrodes, prepared from amorphous $Co_xB_yH_z$ nanoparticles without additives, in 20% KOH solution was tested by means of cyclic voltammetry and chronopotentiometry. Peaks, assigned to hydrogen adsorption and desorption, are observed in the cyclic voltammograms. After charging, hydrogen atoms occupy different types of sites in the substrate, from which electrochemical desorption occurs. An increase in hydrogen content as a result of repeated cycling was established. Discharge capacity of the electrodes, estimated from the chronopotentiometric discharge curves obtained, is about 250 mA h g^{-1}. The observed changes in hydrogen and boron content, due to electrochemical treatment, indicate that the electrode material is an active participant in the whole electrochemical process. Hypotheses for the reaction mechanism are proposed.

Keywords: *$Co_xB_yH_z$ nanoparticles*, *borohydride reduction*, *metal hydride electrodes*

1. Introduction

Nickel–metal hydride (Ni–MH) batteries have become popular as an alternative to the commonly used Ni–Cd system. They possess numerous advantages over Ni–Cd batteries such as absence of toxic Cd, higher energy capacity, high rate capability, tolerance to overcharge and overdischarge, no consumption of electrolyte during charge–discharge cycles and life longer than 1000 charge–discharge cycles. Among their disadvantages are difficulties in preparation of the hydrogen absorbing alloys, used as negative electrode materials, and their high price.

The electrochemical absorption and desorption of hydrogen on some new amorphous materials has been recently reported [1, 2].

Nanoparticles, produced my means of the well-known borohydride reduction method, sorb relatively large amounts of hydrogen during production. For this reason, it was predicted [3] that such nanoparticles would be 'a new route to metal hydrides' for the purposes of Ni–MH batteries.

An electrocatalytic activity of electrodes containing NiB nanosized powders towards the hydrogen evolution reaction (HER) and hydrogenation of some organic compounds has been found [4–8]. The mechanism of these reactions is similar to that of the reaction proceedings on MH electrodes. The electrodes, however, have not been tested for possible battery application.

Various amorphous and nanocrystalline particles have been synthesized by means of the borohydride reduction method, using different preparation techniques developed by Dragieva *et al.* [9–14]. The reduction process is carried out in a reactor at room temperature and atmospheric pressure. A definite volume of solution, containing a determined amount of $NaBH_4$, used as a reductor, is added to another solution of known volume and concentration, containing a salt of a transition metal. Nanoparticles with different hydrogen and boron content were obtained by variation of the salts, solutions concentration, time of mixing and pH. It was established [10, 11] that the total amount of hydrogen in the nanoparticles increased with decrease in boron content. Thus, under appropriate conditions, materials with relatively high and controllable hydrogen content could be produced.

Boron atoms in two states have been observed by X-ray photoelectron spectroscopy in amorphous $Co_xB_yH_z$ nanoparticles [15]. It was assumed that these two states of boron are responsible for the catalytic properties of such powders towards reactions with participation of transition metals, hydrogen and oxygen, taking place on solid–gas or solid–liquid phase boundaries. The appearance of two peaks in the 1s photoelectron spectra of boron was also observed in an amorphous boron-containing alloy [16], exhibiting catalytic activity [17, 18], as well as in amorphous metallic ribbons used in the assembling of torroidal transformers [19].

In our initial study [20], the electrochemical performance of different nanoparticles synthesized by borohydride reduction was tested in alkaline media.

Electrodes were prepared by technology developed for MH electrodes [21]. A predetermined amount of nanoparticles was mixed with teflonized carbon (Vulcan XC-72), used as a binder, and the mixture was pressed onto a current collector (nickel mesh) at room temperature. Several charge/discharge cycles were carried out for each electrode. Discharge capacities higher than 200 mA h g^{-1} were obtained for most of the electrodes. These results, compared with the capacities of commercially used MH electrodes, were encouraging.

The purpose of the present work is to elucidate the performance of nanoparticles prepared by borohydride reduction as active electrode materials in alkaline electrolytes for their possible application to rechargeable batteries. Single-metal $Co_xB_yH_z$ nanoparticles were used as a model system. Electrodes fabricated only from nanoparticles without additives were studied

2. Experimental details

Nanoparticles were synthesized by reduction of aqueous $CoSO_4$ solution (112.44 g dm^{-3}) with a solution of $NaBH_4$ (46.11 g dm^{-3}). The process was carried out in a vertical 'Y'-type reactor at room temperature and atmospheric pressure. Both solutions were simultaneously injected at the same level in the upper part of the reactor and pH was adjusted to 6.7. The reaction time was 10.5 min. The powder obtained was separated from the solution by filtration and dried under vacuum for 24 h. It consisted of nanoscale particles with an amorphous structure [10]. The boron content, analysed titrimetrically [9, 11], was 7.66 wt % and that of hydrogen, determined by gaseous analysis [11], was 0.574 wt %.

Cylindrical electrodes with diameter 6 mm and thickness 2 mm were prepared by pressing about 0.2 g of the powder under pressure of 100 Mpa. The prepared samples were sintered at 200 or 300 °C under a nitrogen atmosphere for 10 min. Such thermal treatment does not change the initial structure of the material, as the crystallization of amorphous $Co_xB_yH_z$ nanoparticles occurs at higher temperatures [14].

The electrochemical experiments were performed in a three electrode H-shape cell with separate compartments for the working and counter electrode. The measurements were carried out in 20% KOH aqueous solution. A large nickel foil was used as a counter electrode. The working electrode potential was measured against a Hg/HgO reference electrode. The experiments were performed using PJT 35-2 potentiostat-galvanostat (Radiometer-Tacussel, France) with an *IMT* 101 electrochemical interface and Volta Master 2 software. Ohmic drop compensation was applied.

Cyclic voltammetry was carried out in the potential range between −1.2 and −0.5 V vs Hg/HgO, starting from the open circuit potential, E_{oc}, and shifting the potential initially in a negative direction.

Totally charged electrodes were discharged at a constant current density of 50 mA g^{-1} up to a cut-off potential of −0.5 V vs Hg/HgO. The discharge capacity of the electrodes was estimated from the chronopotentiograms obtained.

3. Results and discussion

Typical cyclic voltammograms obtained with the investigated $Co_xB_yH_z$ electrodes are shown in Fig. 1. Only an anodic peak is observed on the voltammograms during the first cycle. A cathodic peak begins to appear during the next cycles at potentials more positive than those at which hydrogen evolution occurs. Although the cathodic peak potential is relatively permanent, the anodic peak usually shifts towards more positive potentials after the first few cycles. Both anodic and cathodic peak heights, as well as the integrated areas under anodic and cathodic waves, presented in Fig. 2, develop gradually in each subsequent cycle until permanent values are maintained. The estimated values of anodic and cathodic Tafel slopes are close to 118 mV dec^{-1} (with deviation of ±15 mV dec^{-1}) for all electrodes tested, which is typical for one-electron reactions.

The change in the cathodic switching potential from −1.2 to −1.1 and −1.0 V induces division of the broad anodic wave into two smaller maxima situated at more negative potentials, as seen from Fig. 3(a). Obviously, oxidation reactions having close, but different, redox potentials take place and form the complex anodic peaks observed. After several cycles the anodic waves unify their forms and shift towards more positive potentials, as shown in Fig. 3(b). When the switching potential is more positive than the cathodic peak potential, the height of the corresponding anodic peak sufficiently decreases. If the potential is swept only in the positive region towards the open circuit potential, E_{oc}, the anodic peak disappears

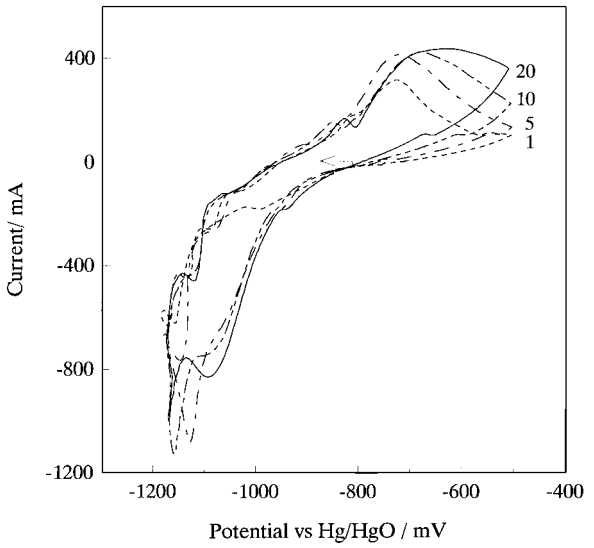

Fig. 1. Cyclic voltammograms of $Co_xB_yH_z$ electrode sintered at 300 °C. Sweep rate 5 mV s^{-1}; 20% KOH solution. Figures inside note the cycle number.

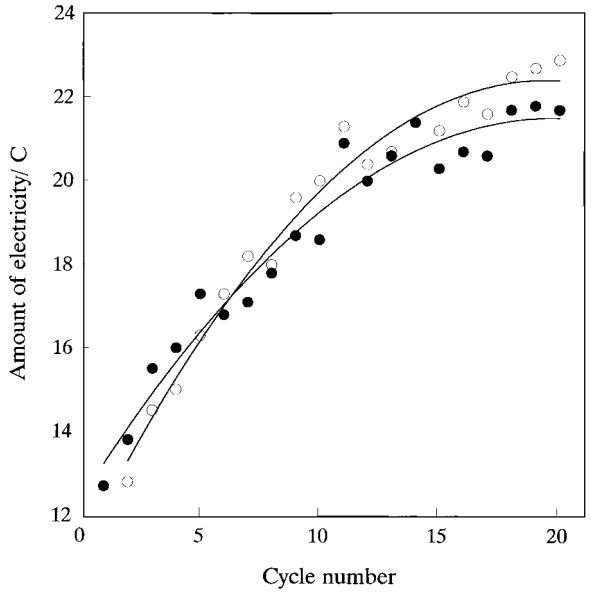

Fig. 2. Amount of electricity estimated by integrating the area under cathodic (○) and anodic (●) peaks in cyclic voltammograms obtained with $Co_xB_yH_z$ electrode sintered at 300 °C. Sweep rate 5 mV s^{-1}; 20% KOH solution.

during the second and subsequent cycles, as shown in Fig. 4. These results indicate that the anodic maxima observed on the cyclic voltammograms are related to the cathodic peak.

Increasing the potential sweep rate induces a larger separation between cathodic and anodic peaks, as seen from Fig. 5, which is an indication of a quasi-reversible electrochemical process.

Considering the presence of hydrogen in the nanoparticles we assume that the observed electrochemical performance is due to oxidation and reduction of hydrogen taking place through a mechanism proposed for hydrogen-sorbing materials [22]. The sorbed hydrogen oxidizes during the first cycle of the voltammetric experiment, which results in the appearance of an anodic peak on the corresponding cyclic voltammogram, presented in Fig. 1. The disturbed equilibrium begins to be restored during the next cycle by electroreduction of water to H_{ads}, taking place via the well-known Volmer reaction, followed by absorption and diffusion of hydrogen atoms into the bulk, with possible formation of a hydride. These phenomena correspond to the appearance of a cathodic peak in the patterns, which is absent during the first cycle.

The existence of a broad anodic wave or two anodic maxima in the studied potential range may be interpreted in the framework of the site distribution model for hydrogen storage in amorphous materials [23]. Water electroreduction occurs at highly electrocatalytic sites at the surface. After charging, hydrogen atoms diffuse into the bulk trying to occupy sites with lower energies, that is, to achieve a more stable state. As seen from Fig. 1, except the sites from which desorption of initially sorbed hydrogen takes place, additional amount of hydrogen atoms occupy new sites and form stronger bonds with the electrode

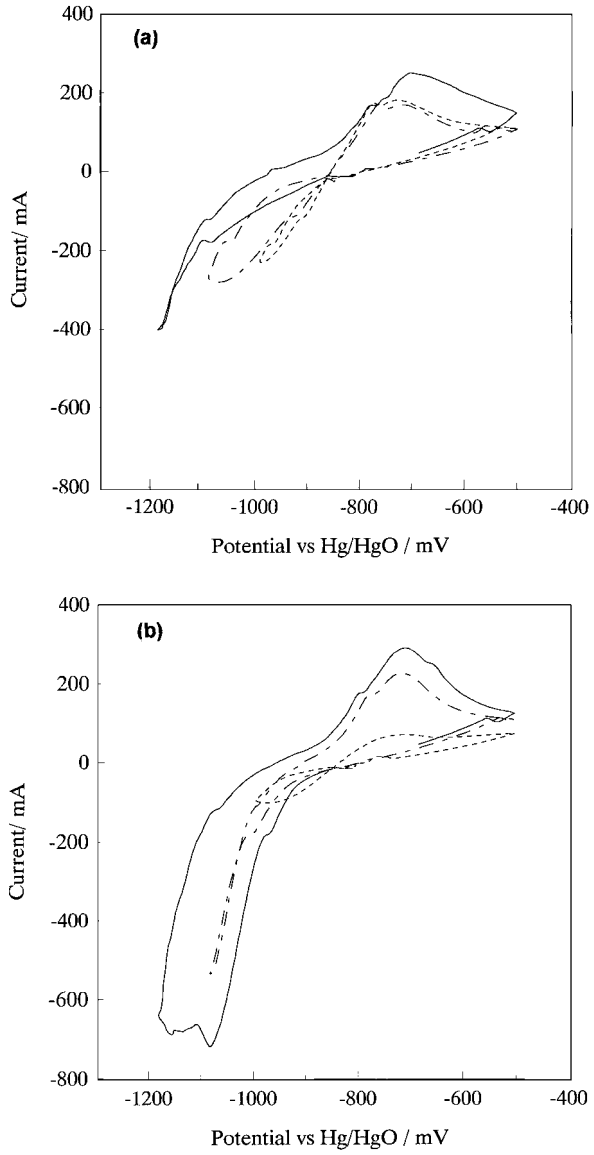

Fig. 3. Cyclic voltammograms of $Co_xB_yH_z$ electrode sintered at 200 °C with different cathodic switching potentials. Sweep rate 5 mV s^{-1}; 20% KOH solution: (a) 1st cycle and (b) 5th cycle.

material as a result of the electrical force applied. The voltammogram pattern changes until equilibration of the population occurs.

The amount of charge passed during discharge is proportional to the hydrogen content in the electrode material. Therefore, the ratio between the charge estimated by integrating the area under the anodic wave in a given cycle and that obtained in the first cycle may be used to evaluate the change in hydrogen content. An increase in the ratio up to a constant value of about 1.7 in the last cycles is obtained, from Fig. 2. This shows that an electrochemical activation of the electrodes can be achieved by repeated cycling.

Such activation (30 cycles) of the samples was carried out in the range −1.2 and −0.5 V vs Hg/HgO at a sweep rate of 5 mV s^{-1} and the electrodes were then charged at constant current density. After charging, the open circuit potential shifted about 100 mV negatively. Such a shift in E_{oc} was predicted

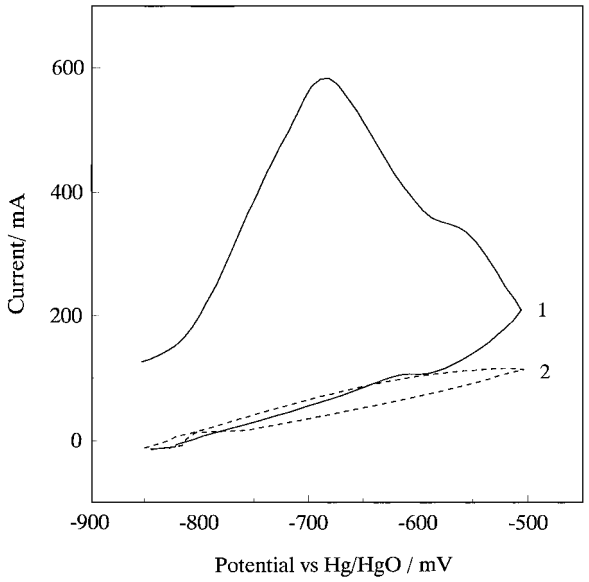

Fig. 4. Cyclic voltammograms of $Co_xB_yH_z$ electrode sintered at 200 °C; the potential is swept only in the positive region towards the open circuit potential, E_{oc}. Sweep rate 10 mV s^{-1}; 20% KOH solution.

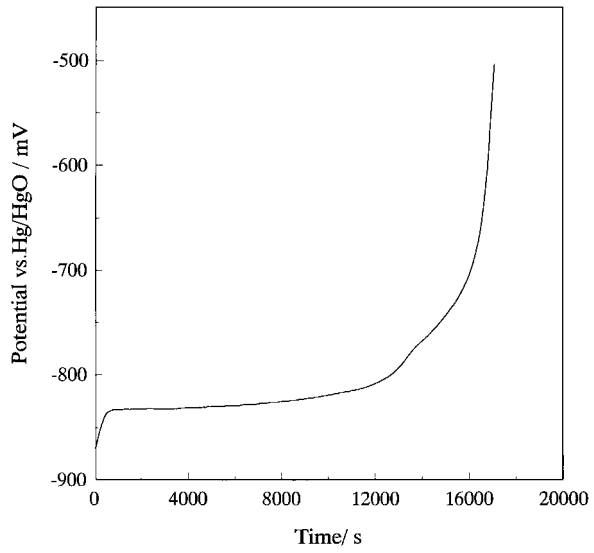

Fig. 6. Chronopotentiometric discharge curve for $Co_xB_yH_z$ electrode sintered at 300 °C. Discharge current density 50 mA g^{-1}.

by simulation [22] and observed experimentally [24] for hydrogen-sorbing materials.

Totally charged electrodes were discharged at constant current and the changes in potential with time were recorded. A typical discharge curve is presented in Fig. 6. The flat plateau observed may be associated with oxidation of adsorbed hydrogen atoms. The consumption of the latter produces diffusion of hydrogen atoms from the bulk electrode to the surface. When the rate of diffusion becomes smaller than that of the electron transfer step, electrochemical desorption begins to occur from lower energy sites and the potential shifts positively.

The discharge capacity estimated from the chronopotentiograms obtained is 250 ± 10 mA h g^{-1}, which is equivalent to oxidation of 1.7 mmol hydrogen per gram electrode material. This amount exceeds the initial hydrogen content in the powder by about 70%. Such an increase in hydrogen content is in a good agreement with the value estimated from the cyclic voltammetry. Obviously, the increase in hydrogen in the electrodes tested is due to the electrochemical charging performed. Almost an equivalent reduction in boron content (0.8 mmol per g) after the electrochemical treatment was determined [25]. It may be assumed that electrochemical charging causes a competition between hydrogen and boron atoms for occupation of available sites in the metallic host, similar to that during nanoparticle production [10]. Thus, the hydrogen storage probably occurs by exchange with boron atoms.

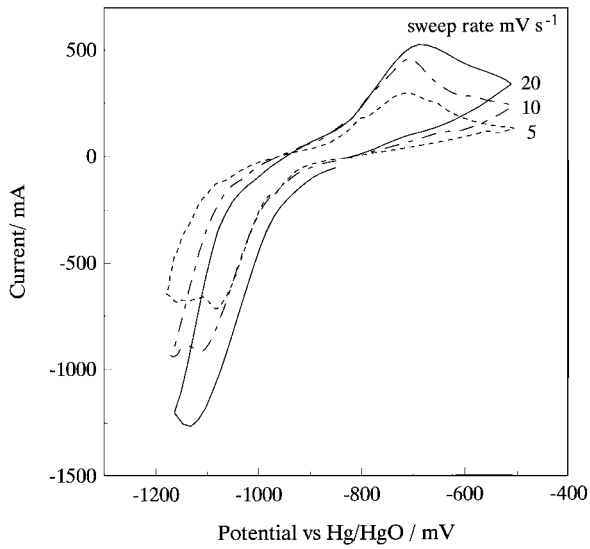

Fig. 5. Cyclic voltammograms of $Co_xB_yH_z$ electrode sintered at 200 °C with different potential sweep rates.

4. Conclusions

The electrochemical performance of electrodes prepared from amorphous $Co_xB_yH_z$ nanoparticles without additives in a strong potassium hydroxide solution was studied.

Cathodic and anodic peaks assigned to electrochemical adsorption and desorption of hydrogen, respectively, were observed on the cyclic voltammograms obtained. The repeated cycling led to an increase in hydrogen content, may be used as an activation procedure. A similar increase in hydrogen content was obtained from the discharge chronopotentiograms recorded. The almost equal decrease in boron content, determined after electrochemical treatment, indicates a possible exchange of boron with hydrogen atoms in the metallic host.

Although nanoparticles were chosen as a model system to elucidate the electrochemical performance and possibility for battery application of these materials, the relatively large values of the discharge capacity obtained suggest the potential for practical use.

References

[1] M. Ciureanu, Q. M. Yang, D. H. Ryan and J. O. Strom-Olsen, *J. Electrochem. Soc.* **141** (1994) 2430.
[2] I. Paseka, *Electrochim. Acta* **40** (1995) 1633.
[3] D. W. Murphy, S. M. Zahurak, B. Vyas, M. Thomas, M. E. Badding and W. C. Fang, *Chem. Mater.* **5** (1993) 767.
[4] P. Los and A. Lasia, *J. Electroanal. Chem.* **333** (1992) 115.
[5] J. J. Borodzinski and A. Lasia, *Int. J. Hydrogen Energy* **18** (1993) 985.
[6] J. J. Borodzinski and A. Lasia, *J. Appl. Electrochem.* **24** (1994) 1267.
[7] B. Mahdavi, P. Los, M. J. Lessard and J. Lessard, *Can. J. Chem.* **72** (1994) 2268
[8] B. Mahdavi, P. Chambrion, J. Binette, E. Martel and J. Lessard, *Can. J. Chem.*, **73** (1995) 846.
[9] I. Dragieva, G. Gavrilov, D. Buchkov and M. Slavcheva, *J. Less-Common Met.* **67** (1979) 375.
[10] I. Dragieva, *in* Dr. Sci. Thesis, 'Amorphous Metal Magnetic Powders Obtained by Borohydride Reduction Process' (1992), Sofia, Bulgaria.
[11] I. Dragieva, Kr. Russev and M. Stanimirova, *J. Less-Common Met.* **158** (1990) 295.
[12] I. Dragieva, P. Mazdrakov and M. Stanimirova, *IEEE Trans. Magn.* **28** (1992) 3183.
[13] I. Dragieva, D. Mehandjiev, E. Lefterowa, M. Stoycheva and Z. Stoynov, *J. Magn. Magn. Mat.* **140–144** (1995) 455.
[14] E. Lefterova, I. Dragieva, V. Tchanev, D. Mehandjiev and M. Mikhov, *ibid.* **140–144** (1995) 457.
[15] V. Krastev, M. Stoycheva, E. Lefterova, I. Dragieva and Z. Stoynov, *J. Alloys Compd.* **1–2** (1996) 186.
[16] M. Mitov, R. Todorova, S. Manev and A. Popov, *J. Mater. Sci. Lett.* **16** (1997) 1712.
[17] M. Stancheva, S. Manev, D. Lazarov and M. Mitov, *Appl. Catalysis A: General* **135** (1996) L19.
[18] V. Dimitrova, M. Mitov, S. Manev and D. Lazarov, *Ann. Sofia Univ.* **89** (1997) 11.
[19] I. Dragieva, Z. Stoynov, I. Nikolaeva and V. Krastev, *J. Solid State Chem.* **133** (1997) 273.
[20] M. Mitov, A. Popov, K. Petrov, I. Dragieva and Z. Stoynov, *in* Proceedings of the National Science Session of the Bulgarian Electrochemical Society (edited by V. Bostanov and N. Atanasov), Sofia (1996), p. 233.
[21] K. Petrov, A. Rostami, A. Visintin and S. Srinivasan, *J. Electrochem. Soc.* **141** (1994) 1747.
[22] A. Lasia and D. Gregoire, *J. Electrochem. Soc.*, **142** (1995) 3393.
[23] R. Kirchheim, M. Kieninger, X. Y. Huang, S. M. Filipek, J. Rush and T. Udovic, *J. Less-Common Met.* **172** (1991) 880.
[24] L. Bai, *J. Electroanal. Chem.* **355** (1993) 37.
[25] I. Dragieva, M. Mitov, A. Popov, Tz. Nishev and Z. Stoynov, *J. Alloys Compd.* (submitted).